Available online at www.sciencedirect.com
SCIENCE DIRECT®
Journal of Solid State Chemistry 176 (2003) 288–293
JOURNAL OF SOLID STATE CHEMISTRY
http://elsevier.com/locate/jssc

Magnetism of the praseodymium halide thiosilicates $Pr_3X[SiS_4]_2$ (X = Cl, Br, I)

Stephan T. Hatscher and Werner Urland*

Institut für Anorganische Chemie, Universität Hannover, Callinstrasse 9, 30167 Hannover, Germany

Received 25 November 2002; received in revised form 12 March 2003; accepted 18 March 2003

Abstract

The magnetism of the three compounds $Pr_3X[SiS_4]_2$ (X = Cl, Br, I) has been measured in the temperature range between 1.7 and 300 K. For the theoretical calculations to interpret the magnetic behavior the angular overlap model was employed to reproduce the ligand field influence and the molecular field approach to take magnetic interaction into account.

Keywords: Magnetism ligand field; Angular overlap model; Thiosilicates; Lanthanide compounds

1. Introduction

Theoretical calculations of the influence of the ligand field on the electronic behavior (i.e., optical, magnetic, etc.) of solid compounds prove to be a versatile tool to obtain information on the strength of interactions of paramagnetic centers with the coordinating ions [1,2]. Several methods are used, one being the angular overlap model (AOM) [3–6]. This semiempirical model is based on the LCAO-MO method. The AOM can be regarded as a ligand field model where local parameters for the molecular central ion–ligand entity are introduced. As the local symmetry and geometry of the paramagnetic center are considered, it is therefore especially suitable for complexes of lower symmetry. It parameterizes the one electron splitting of a partly filled shell in terms of energetic effects of weak covalent bonding/antibonding upon the electronic energies of the central ion [7]. The global ligand field parameters such as Dq, Cp (d-block elements [2]) and B_q^k (f-block elements [8]) are converted to the local angular overlap parameters $e_\sigma(d)$ and $e_\pi(d)$ by taking the crystal structure into account. The empirical parameters $e_\sigma(d)$ and $e_\pi(d)$ estimate the strength of the interaction for a given center–ligand distance (d) and are transferable from one compound to another. The model is equivalent to the superposition model for crystal fields [9,10].

The AOM was used successfully to interpret the electronic behavior of d-block [11–15] as well as f-block elements [8,16–22], and to estimate E and D parameters for ESR spectroscopy [23].

We succeeded in synthesizing the homologue compounds $Ln_3Cl[SiS_4]_2$ (Ln = La–Pr) [24], $Ln_3Br[SiS_4]_2$ (Ln = La–Nd, Sm, Gd) [25], and $La_3I[SiS_4]_2$ (Ln = La, Pr, Nd, Sm, Tb) [26]. All compounds crystallize isotypically in the monoclinc spacegroup $C2/c$ with two crystallographically different lanthanide positions in the unit cell. Fig. 1 displays the view of the structure in the case of $Pr_3Cl[SiS_4]_2$, Fig. 2 shows the different Pr-polyhedra for this compound.

The lanthanide halide thiosilicates are a good choice for a comparison of the influence of one single halide ligand on the magnetic susceptibility of lanthanide ions.

2. Experimental

Finely ground single crystals of $Pr_3X[SiS_4]_2$ (X = Cl, Br, I) were measured with a SQUID magnetometer (MPMS5, Quantum Design) in a temperature range of 1.7–300 K in magnetic fields (H) of 5 and 10 kOe in the cases of $Pr_3Cl[SiS_4]_2$ and $Pr_3I[SiS_4]_2$ and 1 and 5 kOe in the case of $Pr_3Br[SiS_4]_2$, respectively. The preparation of

*Corresponding author. Fax: +49-511-762-19032.
E-mail address: Urland@acc.uni-hannover.de (W. Urland).

0022-4596/03/$ - see front matter © 2003 Elsevier Science (USA). All rights reserved.
doi:10.1016/S0022-4596(03)00176-2

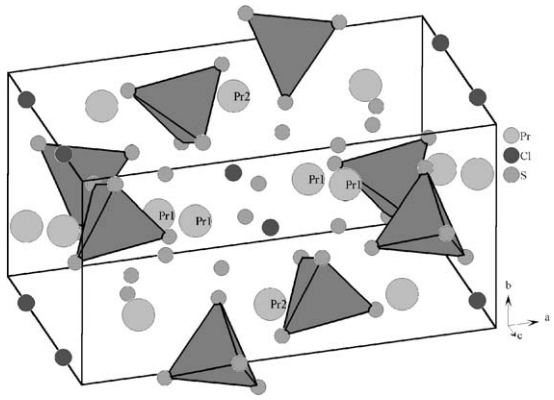

Fig. 1. View on the crystal structure of $Pr_3Cl[SiS_4]_2$ (the silicon ions are hidden in $[SiS_4]$-tetrahedra).

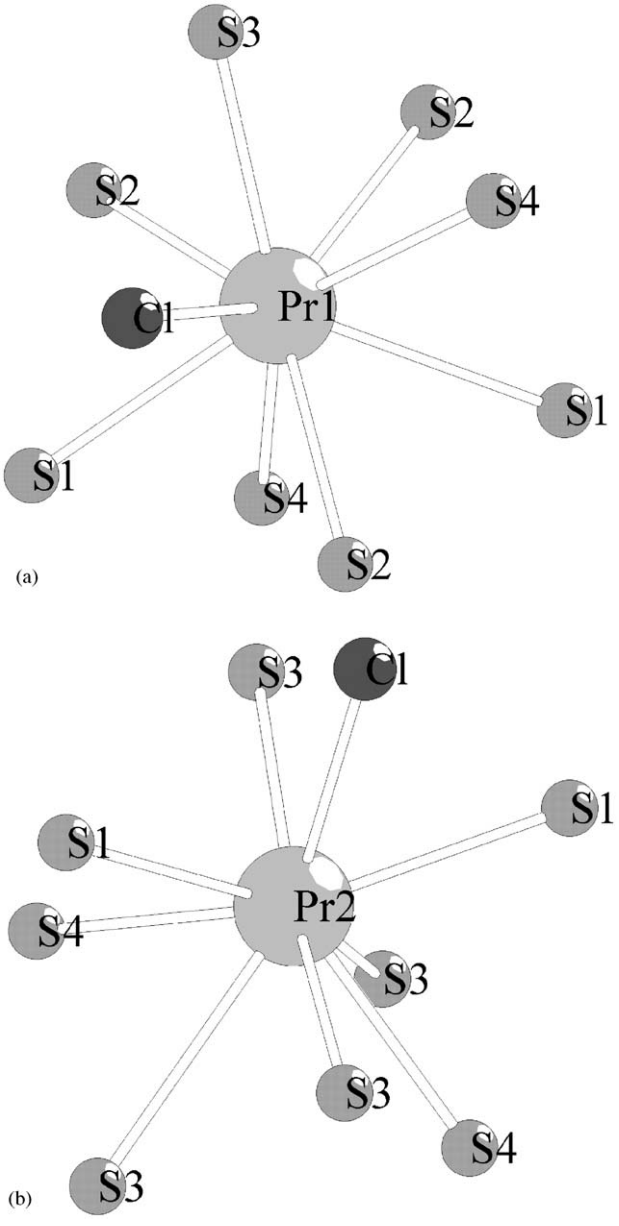

Fig. 2. (a) Coordination of Pr1 and (b) coordination of Pr2.

the crystals is described elsewhere [24–26]. The samples were weighed into the lid of a gelatine capsule. To prevent orientation effects during the measurement, the bottom of the gelatine capsule was pressed on the sample to fix it. A second lid closed the capsule. Then the container was sewed in a plastic straw. The raw magnetic data were corrected for diamagnetism of the sample carrier and of the sample using the increments of Selwood [27].

3. Results

Figs. 3a, 4a and 5a show the measured reciprocal magnetic susceptibility (χ_{mol}^{-1}). Figs. 3b, 4b and 5b show the corresponding magnetic moment (μ) for the title compounds in dependence of temperature ($H = 5$ kOe). No field dependence of the magnetic susceptibility was observed.

For the interpretation of the magnetic behavior, ligand field calculations were employed [8,28,29]. The magnetic susceptibilities of the two crystallographically different praseodymium ions were calculated, taking into account the interelectronic repulsion, the spin orbit coupling, and the crystal field effects using the AOM. The influence of the magnetic field was given by the magnetic field operator $\mu_B H(\boldsymbol{L} + 2 \cdot \boldsymbol{S})$ (μ_B = Bohr Magneton). The calculations have been performed within the 91 $\boldsymbol{L}$, $\boldsymbol{S}$, $\boldsymbol{J}$, $\boldsymbol{M}_J$-states for the f^2-configuration of the Pr^{3+} ion. The basis set used is given in Table 1. The electron–electron interaction parameters (F_2, F_4, F_6) and the spin orbit coupling constant (ζ) were taken from the literature [30] and can also be found in Table 1.

The values for the angular overlap parameters $e_\sigma(d)$ and $e_\pi(d)$ for the interaction between Pr and S were calculated from crystal field parameters of PrS given in the literature [31], and those for the Pr–X (X = Cl, Br, I) interactions were derived from magnetic measurements of $PrCl_3$ [32], $PrBr_3$ [33], and PrI_3 [34]. The $e_\sigma(d)$ and $e_\pi(d)$ parameters are displayed in Table 2. Additionally, all parameters were adapted to the actual distances (d) given in Table 3 by assuming a d^{-7} dependence [35],

$$e_{\lambda,1} d_1^7 = e_{\lambda,2} d_2^7, \quad \lambda = \sigma, \pi. \tag{1}$$

Averaging over the susceptibilities for the two different praseodymium positions (cf. Table 3) led to χ'_{mol}.

As the calculated susceptibilities χ'_{mol} strongly deviated from the experimental ones, magnetic interactions were taken into consideration by the simple molecular field approximation according to [29,36,37]

$$\chi_{mol}^{-1} = (\chi'_{mol})^{-1} - \lambda_{MF}, \tag{2}$$

$$\lambda_{MF} = \frac{2zJ'}{N_A \mu_B^2 g_J^2}, \quad J' = (g_J - 1)^2 J. \tag{3}$$

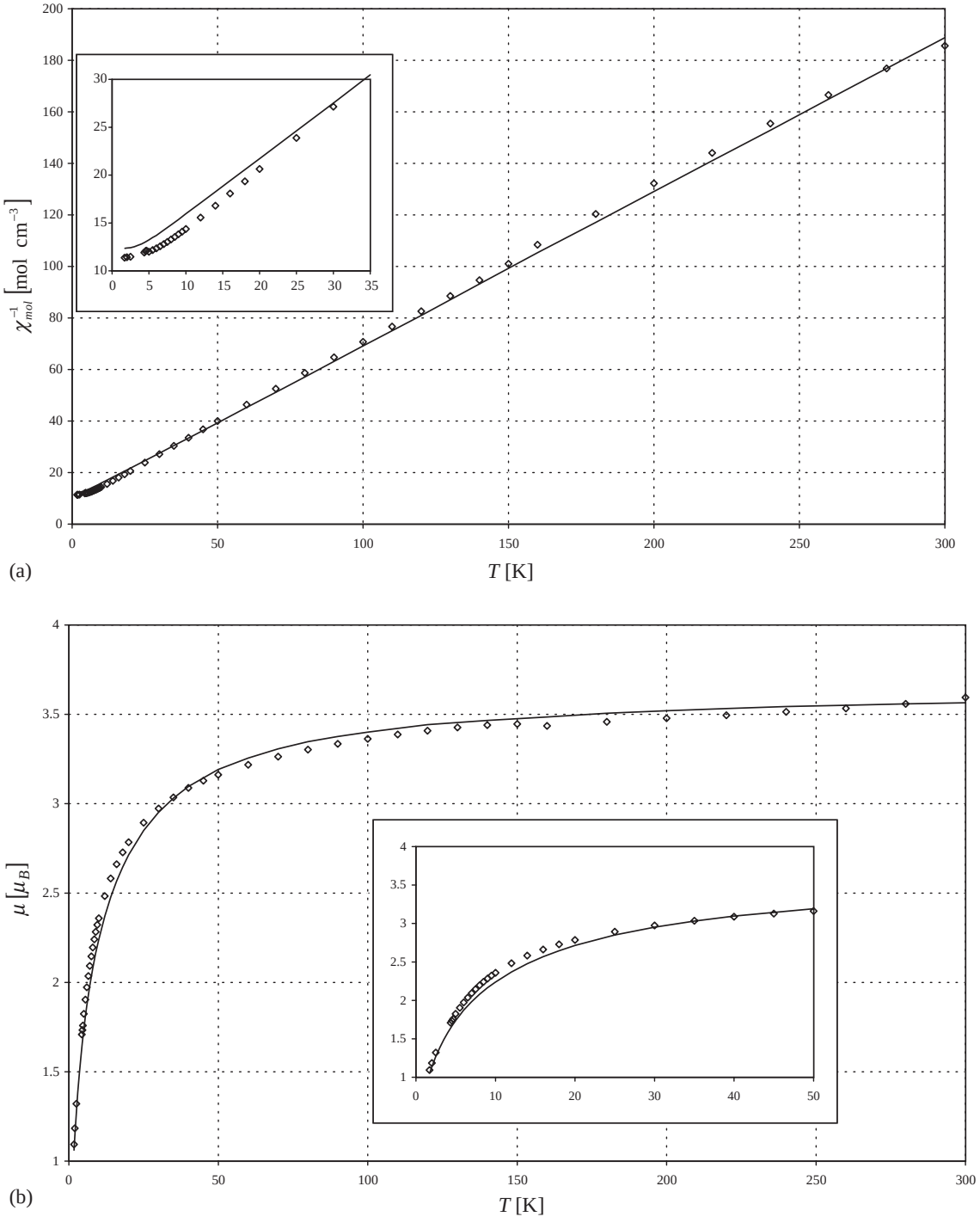

Fig. 3. (a) Comparison of the measured (5 kOe) and calculated reciprocal magnetic susceptibility of $Pr_3Cl[SiS_4]_2$ and (b) comparison of the measured (5 kOe) and calculated magnetic moment of $Pr_3Cl[SiS_4]_2$.

In Eq. (2) the molecular field constant λ_{MF} represents the isotropic part of the magnetic interaction. It is related to the exchange parameter J, resp. J', via Eq. (3). In Eq. (3), N_A represents Avogadro's number, z stands for the number of nearest interacting paramagnetic centers, and g_J is the Landé factor.

The best fittings to the experimentally obtained χ_{mol}^{-1} values (cf. Figs. 3a–5a) were achieved with the data summarized in Table 4. $Pr_3Cl[SiS_4]_2$ shows the largest magnetic interaction, resulting in an overall exchange coupling constant of about $J = -6.25\,cm^{-1}$. With increasing Pr–Pr distances (d') the interaction is decreased to $J = -5.25\,cm^{-1}$ and

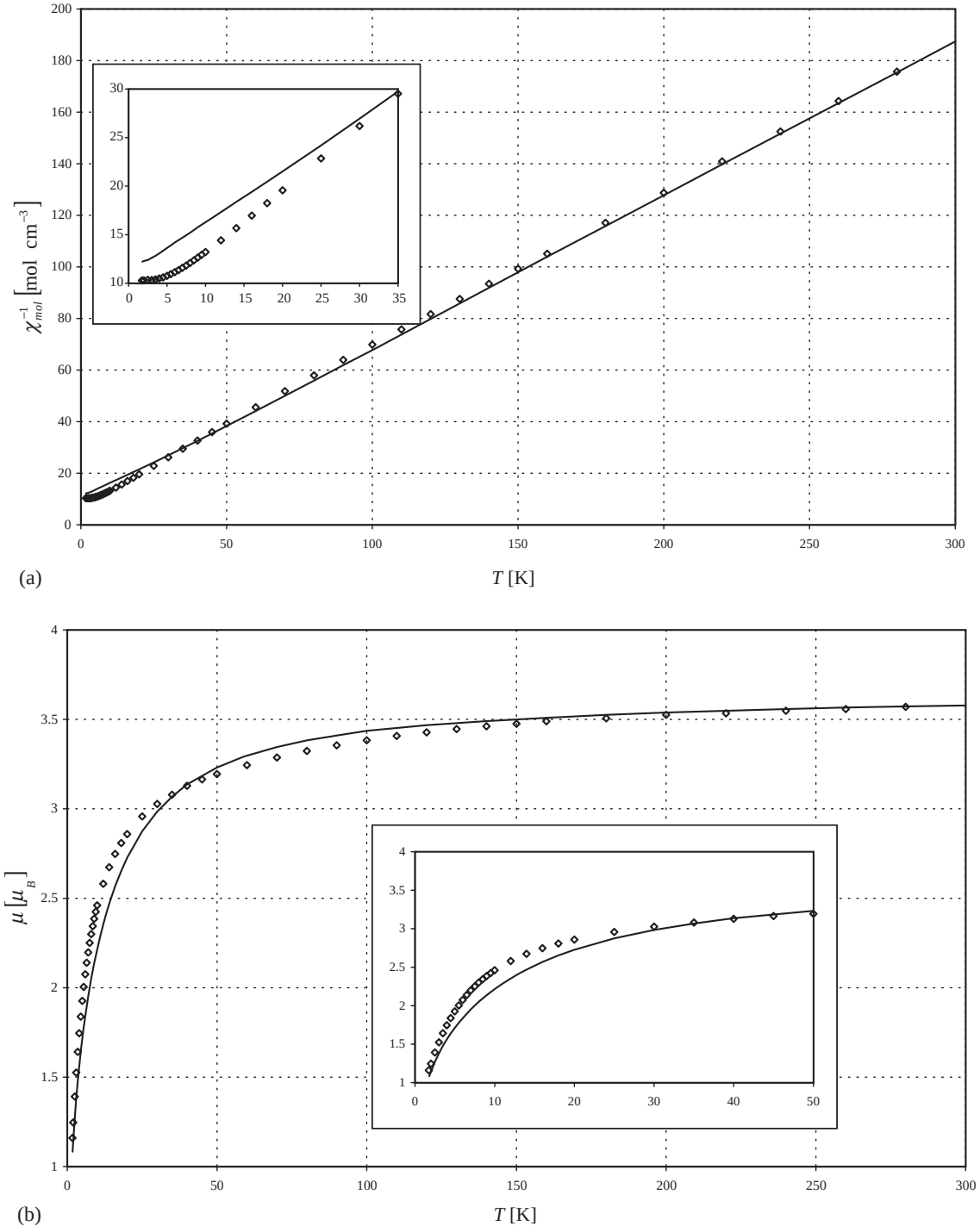

Fig. 4. (a) Comparison of the measured (5 kOe) and calculated reciprocal magnetic susceptibility of $Pr_3Br[SiS_4]_2$ and (b) comparison of the measured (5 kOe) and calculated magnetic moment of $Pr_3Br[SiS_4]_2$.

$-4.25\,cm^{-1}$ for the bromide and the iodide compounds, respectively. The negative signs of the exchange coupling constants indicate antiferromagnetic interaction. It is easy to understand that the interaction should increase with smaller distances between the paramagnetic ions, as it is originated from the overlap of orbitals. The exchange coupling may be understood by a superexchange mechanism via Pr–S–Pr pathways.

The deviations of the experimental curves from the calculated ones (cf. Figs. 3–5) are due to the fact that the molecular field approach is only a rough approximation

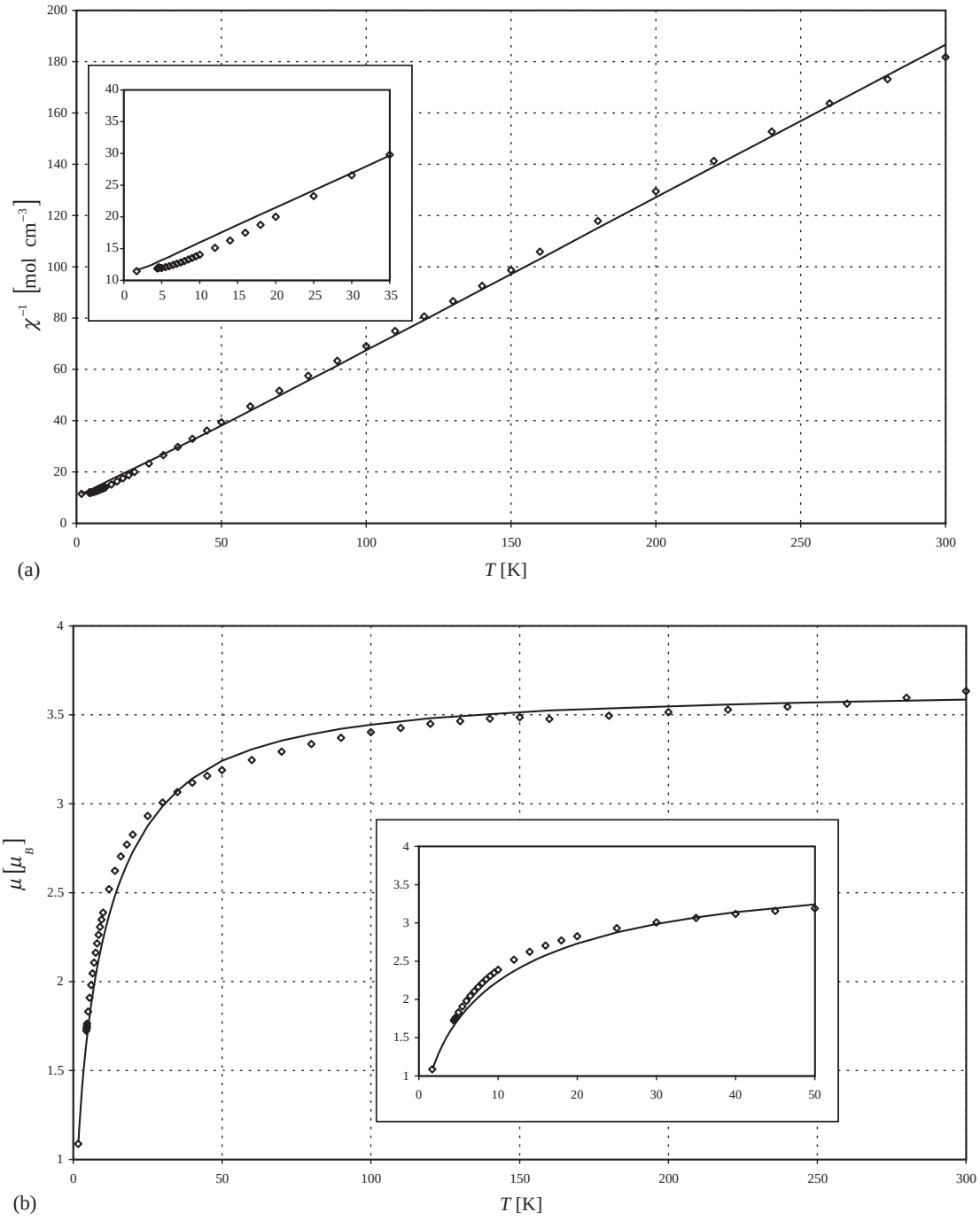

Fig. 5. (a) Comparison of the measured (5 kOe) and calculated reciprocal magnetic susceptibility of $Pr_3I[SiS_4]_2$ and (b) comparison of the measured (5 kOe) and calculated magnetic moment of $Pr_3I[SiS_4]_2$.

Table 1
Parameters F_2, F_4, F_6, ζ [cm^{-1}] and basis set for Pr^{3+} in $Pr_3X[SiS_4]_2$ (X = Cl, Br, I)

Pr^{3+}	F_2	304.5
	F_4	51.88
	F_6	5.321
	ζ	729.5
	Basis set	^3P, ^3F, ^3H, ^1S, ^1D, ^1G, ^1I

Table 2
Values for $e_\sigma(d)$ and $e_\pi(d)$ (cm^{-1}) and distances d (pm) for the interaction of Pr^{3+} with its ligands in $Pr_3X[SiS_4]_2$ (X = Cl, Br, I)

Type of interaction	$e_\sigma(d)$ and $e_\pi(d)$	d
Pr–Cl	455 and 185	273
Pr–Br	213 and 74	304
Pr–I	156 and 42	332
Pr–S	139 and 57	289

Table 3
Interatomic distances (pm) in $Pr_3X[SiS_4]_2$ (X = Cl, Br, I)

	$Pr_3Cl[SiS_4]_2$	$Pr_3Br[SiS_4]_2$	$Pr_3I[SiS_4]_2$
Pr1–S2[a]	289.9(1)	289.8(2)	290.9(2)
Pr1–S4[b]	292.2(1)	290.3(2)	292.6(2)
Pr1–S3[c]	287.6(1)	292.0(2)	294.1(2)
Pr1–S2[d]	303.4(1)	297.8(2)	296.8(2)
Pr1–S4[d]	299.7(1)	301.0(2)	300.6(2)
Pr1–S2[c]	302.0(1)	300.2(2)	301.2(2)
Pr1–S1[e]	294.0(1)	302.1(2)	304.8(2)
Pr1–S1[a]	312.6(2)	310.9(2)	307.7(2)
Pr1–X[f]	330.7(1)	332.4(1)	341.8(2)
Pr2–S4[d,g]	287.9(1)	287.3(2)	288.3(2)
Pr2–S1[a,h]	286.7(1)	287.6(2)	292.2(2)
Pr2–S3[d,g]	329.9(1)	329.1(2)	322.0(3)
Pr2–S3[a,h]	332.8(1)	327.7(2)	328.5(2)
Pr2–X[i]	288.8(2)	306.8(1)	326.1(2)

Symmetry operations: [a] $-x+1/2,-y+1/2,-z+1$, [b] $x,y,z+1$, [c] $x,-y+1,z+1/2$, [d] $-x+1/2,y-1/2,-z+1/2$, [e] $x,-y,z+1/2$, [f] $-x,-y+1,-z+1$, [g] $x+1/2,y-1/2,z+1$, [h] $x+1/2,-y+1/2,z+1/2$, [i] $-x+1/2,-y+3/2,-z+1$.

Table 4
Smallest Pr–Pr distances d' (pm), number of next neighboring paramagnetic centeres z, Landé factor g_J, molecular field constant λ_{MF} ($mol\,cm^{-3}$), and exchange parameters J' and J (cm^{-1}) for $Pr_3X[SiS_4]_2$ (X = Cl, Br, I).

Compound	d'	z	g_J	λ_{MF}	J'	J
$Pr_3Cl[SiS_4]_2$	437.5	2	4/5	6	-2.5×10^{-1}	−6.25
$Pr_3Br[SiS_4]_2$	439.8	2	4/5	5	-2.1×10^{-1}	−5.25
$Pr_3I[SiS_4]_2$	442.2	2	4/5	4	-1.7×10^{-1}	−4.25

of the magnetic interaction of the Pr ions in these compounds.

4. Conclusions

The interpretation of magnetic susceptibility data with the method here employed using the AOM to describe the ligand field influence and the molecular field approach to take magnetic exchange into consideration gives insight into lanthanide–ligand as well as lanthanide–lanthanide interactions.

References

[1] W. Kutzelnigg, Einführung in die Theoretische Chemie, 1. Auflage, Wiley-VCH, Weinheim, 2002.
[2] M. Gerloch, R.C. Slade, Ligand-Field Parameters, Cambridge University Press, Cambridge, 1973.
[3] D.S. McClure, in: S. Kirschner (Ed.), Advances in the Chemistry of Coordination Compounds, McMillan, New York, 1961.
[4] Chr. Klixbüll Jørgensen, R. Pappalardo, H.H. Schmidtke, J. Chem. Phys. 39 (1963) 1422.
[5] C.E. Schäffer, Chr. Klixbüll Jørgensen, Mol. Phys. 9 (1965) 401.
[6] C.E. Schäffer, Struct. Bonding 5 (1968) 68.
[7] P.J. Steenkamp, Aust. J. Chem. 37 (1984) 679.
[8] W. Urland, Chem. Phys. 14 (1976) 393.
[9] D.J. Newman, B. Ng, Rep. Prog. Phys. 52 (1989) 699.
[10] D.J. Newman, B. Ng, Crystal Field Handbook, Cambridge University Press, Cambridge, 2000.
[11] M. Gerloch, Magnetism and Ligand-Field Analysis, Cambridge University Press, Cambridge, London, New York, New Rochelle, Melbourne, Sydney, 1983.
[12] W. Urland, S.R. Niketic, Chem. Phys. Lett. 129 (1986) 592.
[13] A. Bencini, C. Benelli, G. Gatteschi, Coordination Chem. Rev. 60 (1984) 131.
[14] A. Möller, Z. Anorg. Allg. Chem. 628 (2002) 77.
[15] R. Glaum, H. Thauern, A. Schmidt, M. Gerk, Z. Anorg. Allg. Chem. 628 (2002) 2800.
[16] W. Urland, Chem. Phys. Lett. 50 (1977) 445.
[17] K.D. Warren, Inorg. Chem. 16 (1977) 2008.
[18] W. Urland, Chem. Phys. Lett. 53 (1978) 296.
[19] W. Urland, Chem. Phys. Lett. 62 (1979) 525.
[20] A. Becker, W. Urland, J. Alloys Compd. 275–277 (1998) 62.
[21] B.M. Flanagan, P.V. Bernhardt, E.R. Krausz, S.R. Lüthi, M.J. Riley, Inorg. Chem. 40 (2001) 5401.
[22] B.M. Flanagan, P.V. Bernhardt, E.R. Krausz, S.R. Lüthi, M.J. Riley, Inorg. Chem. 41 (2002) 5024.
[23] A. Bencini, I. Ciofini, M.G. Uytterhoeven, Inorg. Chim. Acta 274 (1998) 90.
[24] S.T. Hatscher, W. Urland, Mater. Res. Bull. 37 (2002) 1239.
[25] S.T. Hatscher, W. Urland, Z. Anorg. Allg. Chem. 628 (2002) 608.
[26] S.T. Hatscher, W. Urland, Z. Anorg. Allg. Chem. 627 (2001) 2198.
[27] P.W. Selwood, Magnetochemistry, Interscience Publishers, New York, London, Sydney, 1956.
[28] W. Urland, Chem. Phys. Lett. 46 (1977) 457.
[29] H. Lueken, Magnetochemie, Teubner-Verlag, Stuttgart, Leipzig, 1999.
[30] J.S. Margolis, J. Chem. Phys. 35 (1961) 1367.
[31] K.C. Turberfield, L. Passell, R.J. Birgeneau, E. Bucher, Phys. Rev. Lett. 25 (1970) 752.
[32] W. Urland, Chem. Phys. Lett. 83 (1981) 116.
[33] W. Urland, unpublished results.
[34] W. Urland, unpublished results.
[35] W. Urland, Chem. Phys. 38 (1979) 407.
[36] B. Bleaney, Proc. Roy. Soc. London Sect. A 276 (1963) 19.
[37] W. Urland, Z. Naturforsch. 35a (1980) 247.